Microsystem Technologies (2019) 25:1243–1250
https://doi.org/10.1007/s00542-018-4157-y

TECHNICAL PAPER

Analysis of non-linear radiative stagnation point flow of Carreau fluid with homogeneous-heterogeneous reactions

T. Hayat[1,2] · Ikram Ullah[1] · M. Farooq[3] · A. Alsaedi[2]

Received: 29 May 2018 / Accepted: 27 September 2018 / Published online: 13 October 2018

Abstract

Current work focuses on stagnation point flow of MHD Carreau fluid with heterogeneous–homogeneous reactions. Nonlinear stretched sheet of variable thickness is the main agent for flow induction. Liquid is assumed an electrically conducted. Nonlinear thermal radiation and heat generation/absorption aspects are addressed. Proper transformations lead to dimensionless the governing problem. Resultant systems are tackled numerically via NDSolve based Shooting scheme. Importance of emerging variables is addressed through graphical illustrations. Tables regarding the estimations of skin friction and rate of heat transfer are computed and examined for various physical variables. It is found that convective and radiation variables improve the liquid temperature. Obtained outcomes are also compared in limiting way and found an excellent agreement.

1 Introduction

There is a wide range of chemical reactions in nature which have widespread practical applications. These reactions are involved in various processes especially in fog formation and dispersion, food processing, hydrometallurgical industry, air and water pollutions, atmospheric flows, fibres insulation and crops damage due to freezing etc. In these process the molecular diffusion of species on the boundary or inside the chemical reaction is very intricate. Some of the reactions have the capacity to proceed gradually or do not react at the moment with out catalyst. In this direction (Merkin 1996) studied a model for isothermal homogeneous–heterogeneous reactions in boundary layer flow over a flat plate. Forced convection stagnation point flow of viscous fluid with homogeneous–heterogeneous reactions was explored by (Chaudhary and Merkin 1995). (Khan and Pop 2015) put forward such effects on the flow of viscoelastic fluid towards a stretching sheet. The boundary layer flow of Maxwell fluid over a stretching surface with homogeneous-heterogeneous reactions was examined by Hayat et al. (2015a). The characteristics of homogeneous–heterogeneous reactions in the region of stagnation point flow of carbon nanotubes over a stretching cylinder with Newtonian heating was presented by Hayat et al. (2015b). (Farooq et al. 2015) discussed the homogeneous–heterogeneous reaction in flow of Jeffrey liquid. Aspects of homogeneous–heterogeneous reactions in flow of Sisko liquid was studied by Hayat et al. (2018a). Temperature based heat source and nonlinear radiative flow of third grade liquid with homogeneous-heterogeneous reactions is explored by Hayat et al. (2018b).

Heat transport and flow phenomena because of stretching surface have various practical uses in technological and engineering processes. Such phenomenon encountered in paper production, fiber production, extrusion of polymer and metal, wire drawing, hot rolling, refrigeration and heat conduction in tissues etc. Both stretching and kinematics of heat transport during such procedure have a crucial consequence on standard of final outcomes. Initially (Sakiadis 1961) provided the study of boundary layer flow bounded by a stretching sheet. (Crane 1970) and (Gupta and Gupta 1977) inspected heat/mass transport analysis over a stretching sheet with constant surface temperature. Afterwards several theoretical attempts have been performed by several researchers (Bhattacharyya 2011; Turkyilmazoglu

✉ Ikram Ullah
ikramullah@math.qau.edu.pk

[1] Department of Mathematics, Quaid-I-Azam University 45320, Islamabad 44000, Pakistan

[2] Nonlinear Analysis and Applied Mathematics (NAAM) Research Group, Faculty of Science, King Abdulaziz University, P. O. Box 80203, Jeddah 21589, Saudi Arabia

[3] Department of Mathematics, Riphah International University, Islamabad 44000, Pakistan

2011; Malvandi et al. 2014; Shehzad et al. 2015; Hayat et al. 2016a; Ibrahim et al. 2013; Hayat et al. 2016b; Meraj et al. 2017; Zhu et al. 2017; Mahanthesh et al. 2016; Abbasi et al. 2016; Hayat et al. 2017a, b; Sheikholeslami and Shehzad 2017; Hayat et al. 2018c). Further, the stretching sheet with variable thickness occur in practical uses more frequently than a flat sheet. Such flow phenomenon are used in marine structures, aeronautical, mechanical and civil. Variable thickness is used for reduction of structural elements weight and advance way to use material (Shufrin and Eisenberger 2005) Some notable attempts in this direction can be seen via (Fang 2012; Subhashini et al. 2013; Hayat et al. 2015c, 2016c, 2017c, 2018d; Hayat et al. 2018e).

Present study disclose the aspects of homogeneous–heterogeneous reactions and magnetohydrodynamic (MHD) flow of Carreau fluid past a nonlinear starching sheet with variable thickness. It is assumed that plate is heated and exposed to transverse magnetic field. Features of heat generation/absorption and nonlinear thermal radiation are considered in mathematical modeling. Further we imposed convective condition at the surface. Mathematical formulation is constructed through boundary layer and small magnetic Reynolds number assumptions. Resulting nonlinear systems are then attempted numerically by NDSolve technique. Numerical computations and discussion of plots are carried out for various influential variables. Further comparative analysis is provided to validate our current outcomes.

2 Formulation

We intend to inspect steady two-dimensional flow of Carreau fluid in the region of stagnation point flow towards a nonlinear stretching sheet with variable thickness. Liquid is conducting electrically via constant magnetic field of strength B_0 (see Fig. 1). We ignored the contribution of induced magnetic field utilizing the small magnetic Reynolds number assumptions. Let $U_e = U_\infty(x + b_1)^m$ and $U_w = U_0(x + b_1)^m$ indicate the respective velocities of external and sheet flow. Where reference velocities are signified by U_0 and U_∞. Features of radiation and heat generation/absorption are addressed in governing expression. In addition the contribution of homogeneous-heterogeneous reactions are considered. For cubic autocatalysis the homogeneous reaction can be written as (Merkin 1996; Chaudhary and Merkin 1995):

$$A + 2B \rightarrow 3B,\ \ rate = K_c a b^2. \tag{1}$$

On catalyst surface the first-order isothermal reaction is expressed as

$$A \rightarrow B,\ \ rate = K_s a, \tag{2}$$

where a and b the respective concentrations of chemical species A and B and K_c and K_s show the rate constants. Both the reaction processes are assume to be isothermal. The governing expression for flow under consideration are:

$$\frac{\partial u}{\partial x} + \frac{\partial v}{\partial y} = 0, \tag{3}$$

$$\begin{aligned} u\frac{\partial u}{\partial x} + v\frac{\partial u}{\partial y} &= \nu \frac{\partial^2 u}{\partial y^2}\left[1 + \Gamma^2\left(\frac{\partial u}{\partial y}\right)^2\right]^{\frac{n-1}{2}} \\ &\quad + \nu(n-1)\Gamma^2\left(\frac{\partial u}{\partial y}\right)^2 \frac{\partial^2 u}{\partial y^2}\left[1 + \Gamma^2\left(\frac{\partial u}{\partial y}\right)^2\right]^{\frac{n-3}{2}} \\ &\quad + \frac{\sigma B_0^2}{\rho}(U_e - u) + U_e\frac{dU_e}{dx}, \end{aligned} \tag{4}$$

$$u\frac{\partial T}{\partial x} + v\frac{\partial T}{\partial y} = \frac{k}{\rho c_p}\frac{\partial^2 T}{\partial y^2} - \frac{1}{\rho c_p}\frac{16\sigma^*}{3m^*}\frac{\partial}{\partial y}\left(T^3\frac{\partial T}{\partial y}\right) + \frac{Q_0(T - T_\infty)}{\rho c_p}, \tag{5}$$

$$u\frac{\partial a}{\partial x} + v\frac{\partial a}{\partial y} = D_A\frac{\partial^2 a}{\partial y^2} - K_c a b^2, \tag{6}$$

$$u\frac{\partial b}{\partial x} + v\frac{\partial b}{\partial y} = D_B\frac{\partial^2 b}{\partial y^2} + K_c a b^2. \tag{7}$$

$$\left.\begin{aligned} &u = U_w = U_0(x + b_1)^m,\ v = 0,\ -k\tfrac{\partial T}{\partial y} = h_f(T_f - T), \\ &D_A\tfrac{\partial a}{\partial y} = K_s a,\ D_B\tfrac{\partial b}{\partial y} = -K_s a \text{ at } y = A_1(x + b_1)^{\frac{1-m}{2}}, \end{aligned}\right\} \tag{8}$$

$$u \rightarrow U_e = U_\infty(x + b_1)^m,\ T \rightarrow T_\infty,\ a \rightarrow a_0,\ b \rightarrow 0 \text{ as } y \rightarrow \infty, \tag{9}$$

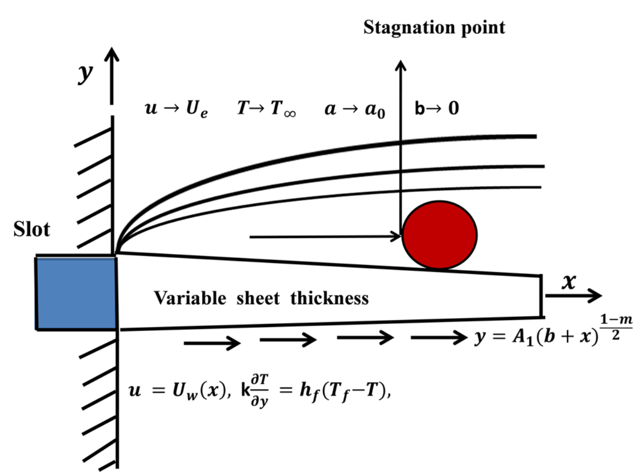

Fig. 1 Schematic flow diagram

where (u, v) denotes the respective velocity components in (x, y) directions, Q_0 the coefficient of heat generation/absorption, $\nu = \frac{\mu}{\rho}$ the kinematic viscosity, ρ the liquid density, Γ the material time constant, μ the dynamic viscosity, k the thermal conductivity, σ the electrical conductivity, m^* the mean absorption coefficient, σ^* the Stefan-Boltzmann constant, b_1 the stretching constant, (D_A, D_B) the diffusion species coefficients of A and B, (a, b) the chemical species of concentration, (T_∞, T) the ambient and surface temperatures and n expresses the power law index. Noted that $n = 1$ corresponds to viscous fluid. The transformations are defined as follow:

$$\left.\begin{array}{l} u = U_0(x+b_1)^m F'(\eta),\ v = -\sqrt{\left(\frac{m+1}{2}\right)\nu U_0(x+b_1)^{m-1}}\left[F(\eta) + \eta F'(\eta)\left(\frac{m-1}{m+1}\right)\right], \\ \eta = y\sqrt{\left(\frac{m+1}{2}\right)\frac{U_0(x+b_1)^{m-1}}{\nu}},\ \theta(\eta) = \frac{T-T_\infty}{T_f-T_\infty},\ g(\eta) = \frac{a}{a_0},\ h(\eta) = \frac{b}{a_0}. \end{array}\right\} \quad (10)$$

On using Eq. (10), the continuity expression is identically satisfied while Eqs. (4, 5, 6, 7, 8, 9) become

$$F'''\left[1 + We^2F''^2\right]^{\frac{n-3}{2}}\left[1 + nWe^2F''^2\right] + FF'' - \left(\frac{2m}{m+1}\right)F'^2 + \left(\frac{2}{m+1}\right)M^2(\lambda - F') + \left(\frac{2m}{m+1}\right)\lambda^2 = 0, \quad (11)$$

$$\left.\begin{array}{l} (1+Rd)\theta'' + Rd[(\Theta_w - 1)^3(3\Theta'^2\Theta'^2 + \Theta^3\Theta'') + 3(\Theta_w - 1)^2(2\Theta'^2\Theta + \Theta^2\Theta'') \\ +3(\Theta_w - 1)(\Theta'^2 + \Theta\Theta'')] + \Pr F\Theta' + \left(\frac{2}{n+1}\right)\Pr\gamma_1\Theta = 0, \end{array}\right\} \quad (12)$$

$$\frac{1}{Sc}g'' + Fg' - \left(\frac{1}{m+1}\right)K_1gh^2 = 0, \quad (13)$$

$$\frac{\delta_1}{Sc}h'' + Fh' + \left(\frac{1}{m+1}\right)K_1gh^2 = 0, \quad (14)$$

$$\left.\begin{array}{l} F(\alpha) = \alpha\left(\frac{1-m}{1+m}\right),\ F'(\alpha) = 1,\ \theta'(\alpha) = -\gamma(1-\theta(\alpha)), \\ g'(\alpha) = K_2g(\alpha),\ \delta_1h'(\alpha) = -K_2h(\alpha), \end{array}\right\} \quad (15)$$

$$F'(\alpha) \to \lambda,\ \theta(\alpha) \to 0,\ g(\alpha) \to 1,\ h(\eta) \to 0 \text{ as } \alpha \to \infty, \quad (16)$$

where prime represents differentiation via η, $\alpha = A\sqrt{\left(\frac{m+1}{2}\right)\frac{U_0}{\nu}}$ the wall thickness parameter and $\eta = \alpha = A\sqrt{\left(\frac{n+1}{2}\right)\frac{U_0}{\nu}}$ indicates the flat surface. By considering

$$F(\eta) = f(\eta - \alpha) = f(\xi), \qquad \Theta(\eta) = \theta(\eta - \alpha) = \theta(\xi),$$

Eqs. 11, 12, 13, 14, 15, 16 reduced to the from

$$f'''\left[1 + We^2f''^2\right]^{\frac{n-3}{2}}\left[1 + nWe^2f''^2\right] + ff'' - \left(\frac{2m}{m+1}\right)f'^2 + \left(\frac{2}{m+1}\right)M^2(\lambda - f') + \left(\frac{2m}{m+1}\right)\lambda^2 = 0, \quad (17)$$

$$\left.\begin{array}{l} (1+Rd)\theta'' + Rd[(\theta_w - 1)^3(3\theta'^2\theta^2 + \theta^3\theta'') + 3(\theta_w - 1)^2(2\theta'^2\theta + \theta^2\theta'') \\ +3(\theta_w - 1)(\theta'^2 + \theta\theta'')] + \Pr f\theta' + \Pr\left(\frac{2}{m+1}\right)\gamma_1\theta = 0, \end{array}\right\} \quad (18)$$

$$\frac{1}{Sc}g'' + fg' - \left(\frac{1}{m+1}\right)K_1 gh^2 = 0, \quad (19)$$

$$\frac{\delta_1}{Sc}h'' + fh' + \left(\frac{1}{m+1}\right)K_1 gh^2 = 0, \quad (20)$$

$$\left.\begin{array}{c} f(0) = \alpha\left(\frac{1-m}{1+m}\right),\ f'(0) = 1,\ \theta'(0) = -\gamma(1-\theta(0)), \\ g'(0) = K_2 g(0),\ \delta_1 h'(0) = -K_2 h(0), \end{array}\right\} \quad (21)$$

$$f'(\infty) \to \lambda,\ \theta(\infty) \to 0,\ g(\infty) \to 1,\ h(\infty) \to 0. \quad (22)$$

Here $Rd\left(=\frac{4\sigma^* T_\infty^3}{km^*}\right)$ the radiation parameter, $\gamma_1\left(=\frac{Q_0}{\rho c_p U_0}\right)$ the heat generation/absorption variable, $\theta_w\left(=\frac{T_f}{T_\infty}\right)$ the temperature parameter, $We\left(=\sqrt{\frac{U_0^3(m+1)(x+b_1)^{3m-1}}{2\nu}}\right)$ the local Weissenberg number, $\gamma\left(=\frac{h_f}{k\sqrt{\frac{2U_0(x+b_1)^{m-1}}{(1+n)\nu}}}\right)$ the Biot number, $M\left(=\frac{\sigma B_0^2}{\rho U_0 (x+b_1)^{m-1}}\right)$ represents the magnetic parameter, $\lambda\left(=\frac{U_\infty}{U_0}\right)$ the velocity ratio, Pr stands for Prandtl number, $K_1\left(=\frac{K_c a_0^2 (x+b_1)}{U_w}\right)$ the measure of the strength of homogeneous reaction, $Sc\left(=\frac{\nu}{D_A}\right)$ the Schmidt number, $\delta_1\left(=\frac{D_B}{D_A}\right)$ the diffusion coefficient ratio, $K_2\left(=\frac{K_s}{D_A}\sqrt{\frac{\nu(x+b_1)}{U_w}}\right)$ the measure of the strength of heterogeneous reaction and prime designates differentiation via ξ.

Here assume that D_B and D_A are equal i.e., $\delta_1 = 1$ and thus:

$$g(\eta) + h(\eta) = 1. \quad (23)$$

Therefore Eqs. 19, 20 yield

$$\frac{1}{Sc}g'' + fg' - K_1 g(1-g)^2 = 0, \quad (24)$$

and

$$g'(0) = K_2 g(0),\ g(\infty) \to 1. \quad (25)$$

The skin friction and Nusselt number are

$$C_{f_x} = \frac{\tau_w}{\rho U_w^2/2},\ Nu_x = \frac{(x+b_1)q_w}{k(T_f - T_\infty)}, \quad (26)$$

where

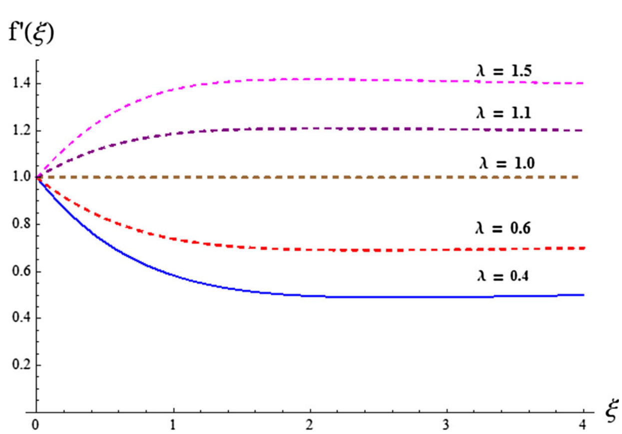

Fig. 2 $f'(\xi)$ through λ

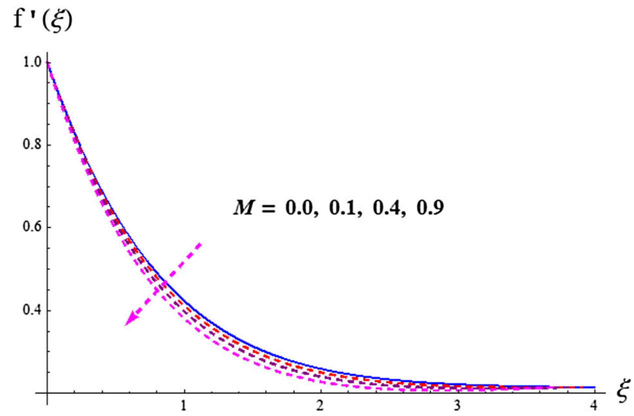

Fig. 3 $f'(\xi)$ through M

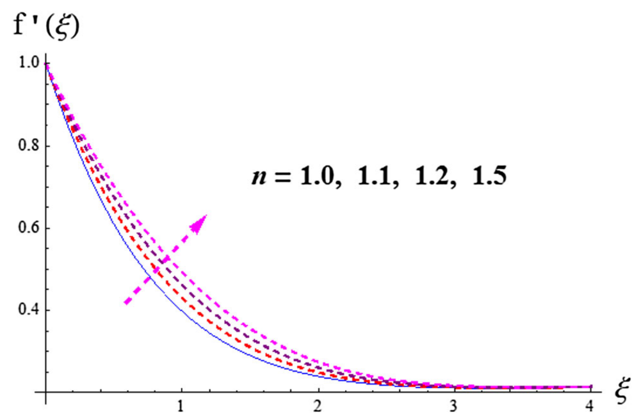

Fig. 4 $f'(\xi)$ through n

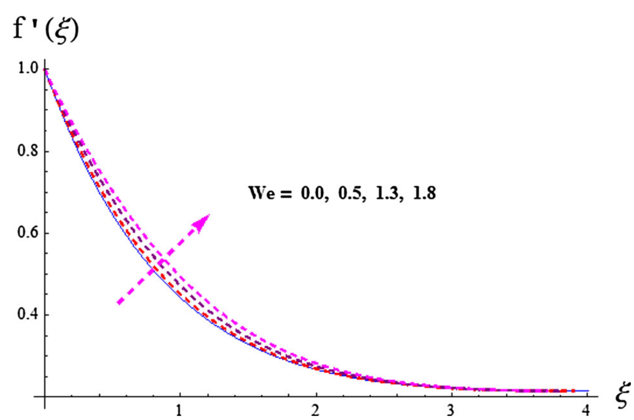

Fig. 5 $f'(\xi)$ through We

$$\left.\begin{array}{l} \tau_w = \eta_0 \frac{\partial u}{\partial y}\left[1 + \Gamma^2\left(\frac{\partial u}{\partial y}\right)^2\right]^{\frac{n-1}{2}}_{y=A_1(x+b_1)^{\frac{1-m}{2}}}, \\ q_w = -k\left(1 + \frac{16\delta^* T^3}{3km^*}\right)\left(\frac{\partial T}{\partial y}\right)_{y=A_1(x+b_1)^{\frac{1-m}{2}}}. \end{array}\right\} \quad (27)$$

Non-dimensional form of skin friction and local Nusselt number are

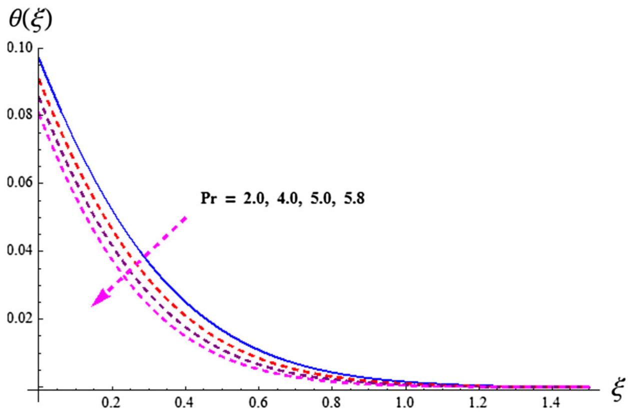

Fig. 6 $\theta(\xi)$ through Pr

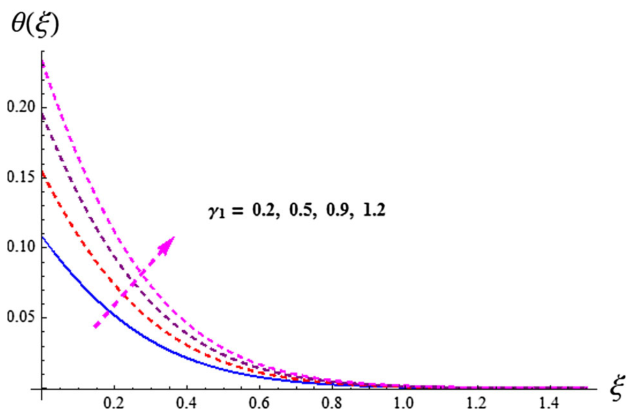

Fig. 7 $\theta(\xi)$ through γ_1

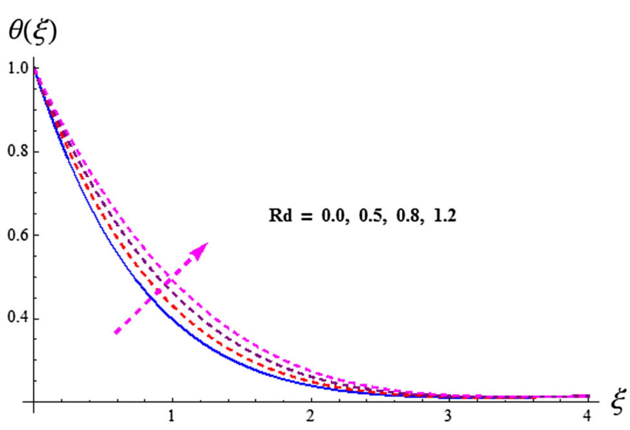

Fig. 8 $\theta(\xi)$ through Rd

$$\left.\begin{array}{l} Re_x^{1/2}C_{f_x} = \sqrt{2(m+1)}\left(f''\left[1+We^2 f''^2\right]^{\frac{n-1}{2}}\right)_{\xi=0}, \\ Re_x^{-1/2}Nu_x = -\sqrt{\left(\frac{m+1}{2}\right)}\left(1+\frac{4}{3}Rd(\theta_w-1)\theta(0))^3\right)\theta'(0), \end{array}\right\} \tag{28}$$

where $Re_x = U_w(x+b_1)^{m+1}/v$ indicates local Reynolds number.

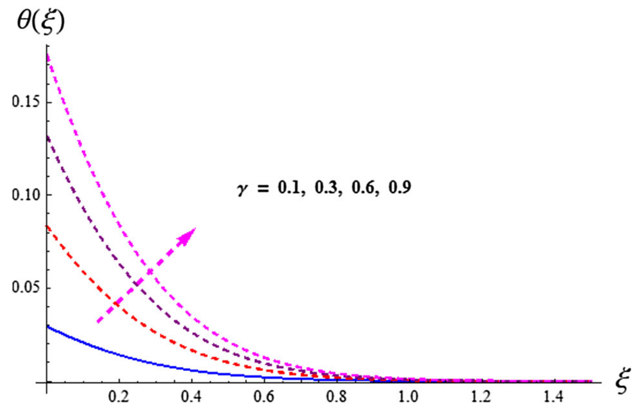

Fig. 9 $\theta(\xi)$ through γ

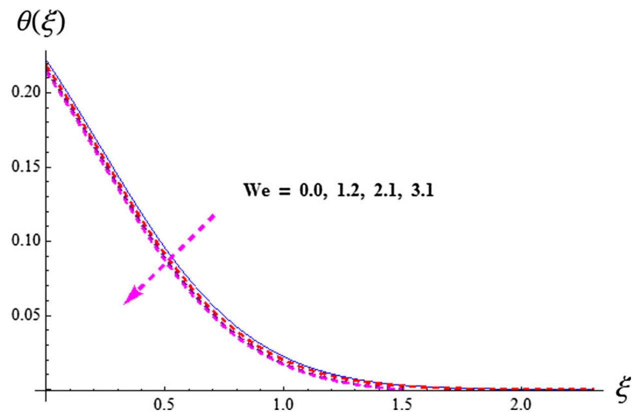

Fig. 10 $\theta(\xi)$ through We

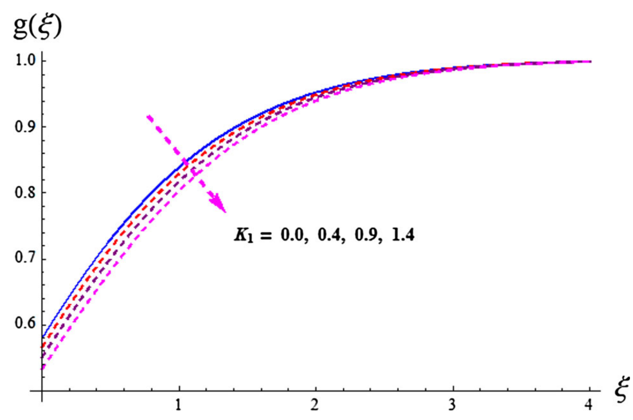

Fig. 11 $g(\xi)$ through K_1

3 Discussion

In order to find the numerical solutions valid locally for Eqs. 17, 18, 19, 20, 21, 22, we employ NDSolve based Shooting technique. Using the numerical technique the interpretations have been performed for numerous estimations of embedded variables. Aspects of λ on $f'(\xi)$ is captured in Fig. 2. Clearly velocity enhances for $\lambda > 1$ but

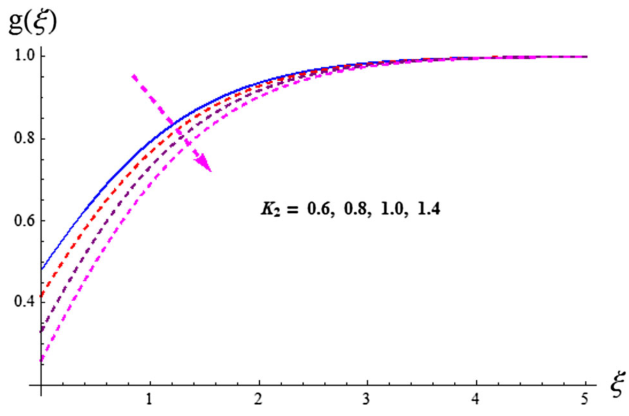

Fig. 12 $g(\xi)$ through K_2

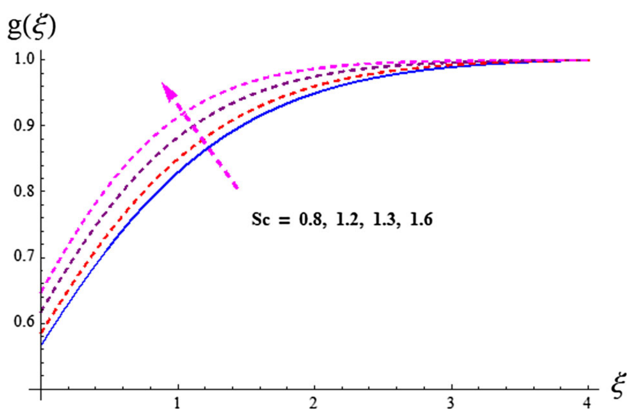

Fig. 13 $g(\xi)$ through Sc

Table 1 Numerical values of skin friction $-Re^{1/2}C_{fx}$ for M, We, λ and m

M	We	λ	m	$-Re^{1/2}C_{f_x}$
0.0	10	0.3	0.5	0.822512
0.5				0.979605
0.9				1.179412
0.3	0.5	0.3	0.5	0.882353
	1.0			0.561191
	1.4			0.440423
0.3	10	0.0	0.5	0.708107
		0.6		0.989598
		1.2		1.39814
0.3	10	0.3	0.5	0.88235
			1.0	0.954615
			1.5	1.019150

for $\lambda < 1$ the layer thickness reduces. Further it is noted that for $\lambda = 1$ there is no boundary layer due to same free stream and velocities. Influence of M on $f'(\xi)$ is disclosed in Fig. 3. Higher M leads to rise the Lorentz forces (resistive forces) which consequently decay the liquid

Table 2 Numerical outcomes of surface temperature gradient $-\theta'(0)$ for different values of γ_1, λ, We, Rd θ_w and γ when $\Pr = 6.2$, $M = \lambda = 0.3$, $m = 0.5$, $n = 1.0$, $K_1 = 0.5 = K_2$ and $Sc = 0.9$.

γ_1	λ	Rd	We	γ	θ_w	$-\sqrt{\frac{m+1}{2}}\theta'(0)$
0.0	0.3	0.3	10	0.3	1.0	0.23253
0.5						0.224449
0.7						0.205668
0.5	0.0	0.3	10	0.3	1.0	0.239721
	0.4					0.237523
	0.7					0.238520
0.5	0.3	0.0	10	0.3	1.0	0.232933
		0.5				0.219102
		1.0				0.206431
0.5	0.3	0.3	0.5	0.3	1.0	0.238231
			1.5			0.238330
			2.5			0.238370
0.5	0.3	0.3		0.1	1.0	0.082281
				0.5		0.342964
				0.8		0.487868
0.5	0.3	0.3	10	0.3	0.5	0.229682
					1.0	0.228521
	0.3	0.3		0.3	1.5	0.227122

Table 3 Comparison for numerical estimations of $-\sqrt{\frac{m+1}{2}}\theta'(0)$ with Hayat et al. (2017) for distinct values of λ and We when $\gamma_1 = Rd = \theta_w = 0$

$-\sqrt{\frac{m+1}{2}}\theta'(0)$			
λ	We	Hayat et al. (2017)	Present study
0.0	10	0.23806	0.238721
0.4		0.23839	0.238123
0.7		0.23870	0.237520
0.2	0.5	0.23823	0.238043
	1.5	0.23833	0.238223
	2.5	0.23837	0.238579

velocity. Figure 4 indicates behavior of n on $f'(\xi)$. It is found that $f'(\xi)$ substantially rise the velocity. Features of We on $f'(\xi)$ is plotted in Fig. 5. As expected, higher We result in an increment of velocity. Variations of Pr on $\theta(\xi)$ is drawn in Fig. 6. Here we see that higher estimations of Pr decay thermal conductivity and thus decline the liquid temperature. Figure 7 exhibits the impact of γ_1 on temperature distributions. This Fig. indicates that thermal field enhances for larger estimations of γ_1. Effects of Rd on $\theta(\xi)$ is declared in Fig. 8. As expected the heat is generated due to radiation process in working liquid which consequently rise the temperature. Temperature for γ is captured in Fig. 9. Clearly $\theta(\xi)$ is enhanced via γ. Figure 10 disclose the impact of We on $\theta(\xi)$. Higher values of We correspond to enhancement of fluid temperature. Figure 11 depicts impact of K_1 on $g(\xi)$. Higher estimations of $K1$ enhance $g(\xi)$. Figure 12 presents effect of K_2 on $g(\xi)$. Here $g(\xi)$ reduces for larger K_2. Behavior of Sc on $g(\xi)$ is noticed in Fig. 13 Decaying feature of $g(\xi)$ is seen for higher Sc. Table 1 reports numerical outcomes of drag force $(-(Re)^{1/2}C_{f_x})$ for distinct flow variables We, M, λ, n and m. It is shown that $-(Re)^{1/2}C_{f_x}$ enhances for n, We, and M. Table 2 is prepared for variations of Nusselt number $-\theta'(0)$ against various embedded variables. It scrutinizes that Nusselt number is enhanced for n, Pr, λ and γ while it diminishes for M. Table 3 certifies the validation of present analysis with limiting study provided by Hayat et al. (2017d). Clearly obtained outcomes are an exellent agreement.

4 Final remarks

Main points include:

- Velocity enhances via We and n while it diminishes through M.
- Temperature field decays through higher Pr and We.
- Thermal layer thickness and temperature are enhanced for higher Rd, γ and γ_1.
- Concentration shows reverse trend for higher estimations of K_2 and K_1.
- Surface drag force enhances via λ, m and M.
- Nusselt number reduces for Rd and θ_w

References

Abbasi FM, Shehzad SA, Hayat T, Ahmad B (2016) Doubly stratified mixed convection flow of Maxwell nanofluid with heat generation/absorption. J Magn Magn Mater 404:159–165

Bhattacharyya K (2011) Boundary layer flow and heat transfer over an exponentially shrinking sheet. Chin Phys Lett 28:074701

Chaudhary MA, Merkin JH (1995) A simple isothermal model for homogeneous-heterogeneous reactions in boundary layer flow: I equal diffusivities. Fluid Dyn Res 16:311–333

Crane LJ (1970) Flow past a stretching plate. Zeitschrift für angewandte Mathematik und Physik ZAMP 21:645

Fang T, Zhang JI, Zhong Y (2012) Boundary layer flow over a stretching sheet with variable thickness. Appl Math Comp 218:7241–7252

Farooq M, Alsaedi A, Hayat T (2015) Note on characteristics of homogeneousheterogeneous reaction in flow of Jeffrey fluid. Appl Math Mech 36(10):1319–1328 **(English edition)**

Gupta PS, Gupta AS (1977) Heat and mass transfer on a stretching sheet with suction or blowing. Can J Chem Eng 55:744–746

Hayat T, Imtiaz M, Almezal S (2015a) Modeling and analysis for three-dimensional flow with homogeneous–heterogeneous reactions. AIP Adv 5:107209

Hayat T, Farooq M, Alsaedi A (2015b) Homogeneous–heterogeneous reactions in the stagnation point flow of carbon nanotubes with Newtonian heating. AIP Adv 5:027130

Hayat T, Farooq M, Alsaedi A, Al-Solamy F (2015c) Impact of Cattaneo-Christov heat flux in the flow over a stretching sheet with variable thickness. AIP Adv 5:087159

Hayat T, Ullah I, Muhammad T, Alsaedi A (2016a) Magnetohydrodynamic (MHD) three-dimensional flow of second grade nanofluid by a convectively heated exponentially stretching surface. J Mol Liq 220:1004–1012

Hayat T, Ullah I, Muhammad T, Alsaedi A, Shehzad SA (2016b) Three-dimensional flow of Powell-Eyring nanofluid with heat and mass flux boundary conditions. Chin Phys B 25:074701

Hayat T, Abbas T, Ayub M, Farooq M, Alsaedi A (2016c) Flow of nanofluid due to convectively heated Riga plate with variable thickness. J Mol Liq 222:854–862

Hayat T, Ullah I, Alsaedi A, Ahmad B (2017a) Radiative flow of Carreau liquid in presence of Newtonian heating and chemical reaction. Result Phys 7(7):15–722

Hayat T, Ullah I, Alsaedi A, Ahmad B (2017b) Modeling tangent hyperbolic nanoliquid flow with heat and mass flux conditions. Eur Phys J Plus 132:112

Hayat T, Ullah I, Alsaedi A, Farooq M (2017c) MHD flow of Powell-Eyring nanofluid over a non-linear stretching sheet with variable thickness. Result Phys 7:189–196

Hayat T, Khan MI, Waqas M, Alsaedi A (2017d) Mathematical modeling of non-Newtonian fluid with chemical aspects: a new formulation and results by numerical technique. Coll Surf A Physicochem Eng Asp 518:263–272

Hayat T, Ullah I, Alsaedi A, Ahmad B (2018a) Numerical simulation for homogeneous–heterogeneous reactions in flow of Sisko fluid. J Br Soc Mech Sci Eng 40:73

Hayat T, Ullah I, Alsaedi A, Ahmad B (2018b) Impact of temperature dependent heat source and nonlinear radiative flow of third grade fluid with chemical aspects. Therm Sci. https://doi.org/10.2298/TSCI180409245H

Hayat T, Ullah I, Alsaedi A, Ahmad B (2018c) Simultaneous effects of non-linear mixed convection and radiative flow due to Riga-plate with double stratification. J Heat Transf 140:102008

Hayat T, Ullah I, Alsaedi A, Waqas M (2018d) Double stratified flow of nanofluid subject to temperature based thermal conductivity and heat source. Thermal Sci. https://doi.org/10.2298/TSCI180121242H

Hayat T, Ullah I, Alsaedi A, Asghar S (2018e) Flow of magneto Williamson nanoliquid towards stretching sheet with variable thickness and double stratification. Radiat Phys Chem 152:151–157

Ibrahim W, Shankar B, Nandeppanavar MM (2013) MHD stagnation point flow and heat transfer due to nanofluid towards a stretching sheet. Int J Heat Mass Transf 56:1–9

Khan WA, Pop I (2015) Effects of homogeneous–heterogeneous reactions on the viscoelastic fluid towards a stretching sheet. J Heat Transf ASME 134:064506

Mahanthesh B, Gireesha BJ, Reddy Gorla RS, Abbasi FM, Shehzad SA (2016) Numerical solutions for magnetohydrodynamic flow of nanofluid over a bidirectional non-linear stretching surface with prescribed surface heat flux boundary. J Magn Magn Mater 417:189–196

Malvandi A, Hedayati F, Ganji D (2014) Slip effects on unsteady stagnation point flow of a nanofluid over a stretching sheet. Powder Technol 253:377–384

Meraj MA, Shehzad SA, Hayat T, Abbasi FM, Alsaedi A (2017) Darcy-Forchheimer flow of variable conductivity Jeffrey liquid with Cattaneo-Christov heat flux theory. Appl Math Mech 38:557–566 **(English edition)**

Merkin JH (1996) A model for isothermal homogeneous-heterogeneous reactions in boundary layer flow. Math Comp Model 24:125–136

Sakiadis BC (1961) Boundary layer behavior on continuous solid surfaces. Am Inst Chem Eng 7:26–28

Shehzad SA, Hussain T, Hayat T, Ramzan M, Alsaedi A (2015) Boundary layer flow of third grade nanofluid with Newtonian heating and viscous dissipation. J Central South Univ 22:360–367

Sheikholeslami M, Shehzad SA (2017) Thermal radiation of ferrofluid in existence of Lorentz forces considering variable viscosity. Int J Heat Mass Transf 109:82–92

Shufrin I, Eisenberger M (2005) Stability of veriable thickness shear deformable plates first order and higher order analysis. Thin Walled Struct 43:189–207

Subhashini SV, Sumathi R, Popb I (2013) Dual solutions in a thermal diffusive flow over a stretching sheet with variable thickness. Int Commun Heat Mass Transf 48:61–66

Turkyilmazoglu M (2011) Multiple solutions of hydromagnetic permeable flow and heat for viscoelastic fluid. J Thermophys Heat Transfer 25:595–605

Zhu J, Wang S, Zheng L, Zhang X (2017) Heat transfer of nanofluids considering nanoparticle migration and second-order slip velocity. Appl Math Mech 38(1):125–136 **(English edition)**